Ad Hoc Networks 9 (2011) 1343–1358

Contents lists available at ScienceDirect

Ad Hoc Networks

journal homepage: www.elsevier.com/locate/adhoc

Comparative analysis of link quality metrics and routing protocols for optimal route construction in wireless mesh networks

Seongkwan Kim [a,*], Okhwan Lee [b], Sunghyun Choi [b], Sung-Ju Lee [c]

[a] System Lab., WiMAX Software R&D Group, Samsung Electronics Co., Ltd., Suwon 443-742, Republic of Korea
[b] School of Electrical Engineering and INMC, Seoul National University, Seoul 151-744, Republic of Korea
[c] Networking & Communications Lab, Hewlett-Packard Laboratories, Palo Alto, CA 94304, United States

ARTICLE INFO

Article history:
Received 18 April 2010
Received in revised form 31 October 2010
Accepted 15 March 2011
Available online 31 March 2011

Keywords:
Wireless mesh network
Routing
Link metric
Interference
End-to-end performance

ABSTRACT

We provide a comparative analysis of various routing strategies that affect the end-to-end performance in wireless mesh networks. We first improve well-known link quality metrics and routing algorithms to enhance performance in wireless mesh environments. We then investigate the *route optimality*, i.e., whether the best end-to-end route with respect to a given link quality metric is established, and its impact on the network performance. Network topologies, number of concurrent flows, and interference types are varied in our evaluation and we find that a non-optimal route is often established because of the routing protocol's misbehavior, inaccurate link metric design, interflow interference, and their interplay. Through extensive simulation analysis, we present insights on how to design wireless link metrics and routing algorithms to enhance the network capacity and provide reliable connectivity.

1. Introduction

Wireless mesh networking is an attractive WLAN (Wireless Local Area Network) solution because of their instant deployability, self-configuring, last-mile broadband access provisioning, and low-cost backhaul services for large coverage. A wireless mesh network is typically composed of mesh (access) points, gateway nodes, and wireless clients. The Internet connection is provided via a few wired gateways. Mesh points, mesh access points, and gateways communicate with each other via wireless medium, and form a wireless backhaul. Wireless clients gain network access via a mesh access point which they associate with.

Providing reliable high-throughput network connectivity to wireless clients is the most important property for wireless mesh networks. To improve the wireless mesh backbone capacity, many areas such as routing, rate adaptation, topology control, and interference management have been investigated. Research on designing a link metric that represents time-varying wireless link quality for wireless mesh routing has been quite active [1,2], whereas the effort to improve the efficiency of utilized routing algorithms has been relatively little. Most (if not all) simply borrow routing algorithms devised for MANET (Mobile Ad hoc Network), and do not provide any synthetic view of the employed routing protocol and link metric combination.

Recently, the IEEE 802.11s working group has been working towards standardizing wireless mesh networking based on IEEE 802.11 WLAN protocols [3]. The 802.11s defines a routing algorithm called HWMP (Hybrid Wireless Mesh Protocol), which can enable a tree-based routing. The core operations however are nearly identical to AODV (Ad hoc On-demand Distance Vector) [4], and the draft itself does not include any detailed analysis of the expected performance, which has not been investigated thoroughly in the literature.

* Corresponding author. Tel.: +82 10 8870 4000.
E-mail addresses: seongkwan@ieee.org (S. Kim), ohlee@mwnl.snu.ac.kr (O. Lee), schoi@snu.ac.kr (S. Choi), sjlee@hp.com (S.-J. Lee).

1570-8705/$ - see front matter © 2011 Published by Elsevier B.V.
doi:10.1016/j.adhoc.2011.03.011

This paper investigates and analyzes various causes that affect *route optimality*. A route is optimal if it achieves the best end-to-end route metric in terms of the given link metric and the route selection criterion. For example, in the case of ETX (Expected Transmission Count) metric and the corresponding route selection criterion, finding the minimum CETX (Cumulative ETX) [1], the generated route can be claimed as optimal when its CETX is the smallest out of all feasible routes from the source to the destination. To this aim, we compare the end-to-end metric and the throughput performance of dynamic routing protocols with an offline routing scheme. We consider the state-of-the-art link quality metrics and routing protocols, and evaluate them in diverse environmental settings in terms of network topology, interference, and number of concurrent flows. We provide a synthetic view of the performance dynamics of wireless mesh networks and the components that impact the performance, each of which cannot give the complete analysis for the network behavior by itself.

In particular, we make the following contributions.

- We improve the well-known link metrics, ETX and ETT (Expected Transmission Time) [2], to better reflect the quality of wireless links than their original designs.
- We revisit AODV and OLSR (Optimized Link State Routing) protocols to support these link quality metrics and to enhance performance in wireless mesh network environments. We choose these routing protocols as the representatives of on-demand and proactive routing algorithms, respectively. Note that they are ratified RFCs (Request For Comments) and have been adopted in the 802.11s drafts.
- An offline routing scheme that builds the optimal path for a given link metric is devised to show the performance upper bound and compare it with those of AODV and OLSR. This helps us have an analytical view to reveal the detailed causes that yield throughput degradation for a given routing strategy.
- We provide a cross-layer analysis by which the TCP performance can be affected by various network operations such as RERR (Route Error) packet generations in AODV, in-series packet collisions occurring in a heavily congested link, and interflow interferences.
- Through extensive ns-2 simulations with various routing strategies, traffic types, number of concurrent flows, and topologies, we discover that a non-optimal route setup frequently occurs because of routing protocols misbehavior, link metric inaccuracy, interflow interference, and their interplay, thus affecting the end-to-end performance. We also provide insights on how to design mesh link metrics and routing algorithms to achieve enhanced network capacity and provide reliable mesh connectivity to wireless clients.

The rest of the paper starts to revisit the state-of-the-art link quality metrics and routing algorithms in Sections 2 and 3. After describing the considered network configurations in Section 4, we explore the impact of network configurations on the end-to-end performance in Sections 5 and 6. Section 7 reviews the related work, and we conclude this paper in Section 8.

2. Link quality metric revisions

We first revisit the original designs of ETX and ETT, and discuss the desired modifications.

2.1. ETX and ETT

ETX is a wireless link metric that was designed to overcome the limitation of HOP (minimum hop count) metric. The ETX of a link is the expected number of (re)transmissions required to successfully send a packet over the link. The derivation of ETX starts from measuring the forward and backward packet delivery ratios over the link. The forward delivery ratio (d_f) is the measured successful transmission probability of data packets received by the recipient. The backward delivery ratio (d_b) is the successful transmission probability of ACK (Acknowledgement) packets measured by the data packet sender. The probability that a transmission is correctly received and acknowledged is $d_f \times d_b$. Assuming that each transmission is independent from previous transmissions, each transmission attempt including retransmissions can be regarded as a Bernoulli trial and the expected transmission count is given by $\mathrm{ETX} = \frac{1}{d_f \times d_b}$.

ETX represents a non-binary quality measure on a wireless link in contrast to the binary HOP. ETX however fails to capture the *multi-rate* capability of the link. d_f and d_b are measured with hello messages transmitting at the lowest rate, while a data packet can be sent at a higher rate. Note that the transmission success probability of fixed-size hello messages cannot be the same as those of actual data packets and 802.11 ACKs. Hence, ETX over a multi-rate link is likely to misestimate the link quality.

ETT is a bandwidth-adjusted ETX; the time spent in transmitting the data packet is multiplied by ETX, i.e., $\mathrm{ETT} = \mathrm{ETX} \times \frac{\ell}{r}$, where ℓ denotes the nominal size of data packets and r is the link rate used for the packet transmissions. While ETT employs the rate information to represent the wireless link quality more precisely than ETX, how to measure ETX (measuring forward and backward delivery ratios via fixed-size and fixed-rate broadcast hello messages) does not change for ETT calculation. Therefore, the original issue of ETX inherently exist with ETT.

2.2. Link metrics of interest

To overcome the aforementioned problems, we consider the multi-rate feature of IEEE 802.11 PHY (Physical layer) along with ETX and ETT. We assume that d_f and d_b are estimated for a given link-rate set $\mathbb{R}$; d_{f,r_i} is the forward delivery ratio with the link rate r_i ($r_i \in \mathbb{R}$) and the nominal size of data packet ℓ, and d_{b,r_i} is for the backward direction, i.e., for ACK transmissions. The best ETX over a wireless link should be the minimum out of all available ETX measures:

$$\mathrm{ETX}^* = \underset{r_i \in \mathbb{R}}{\operatorname{argmin}} \mathrm{ETX}_i, \tag{1}$$

where $\mathrm{ETX}_i = \frac{1}{d_{f,r_i} \times d_{b,r_i}}$. Then, the estimation of ETT employs the modified ETX:

$$\mathrm{ETT}^* = \underset{r_i \in \mathbb{R}}{\operatorname{argmin}} \mathrm{ETX}_i \times \frac{\ell}{r_i}. \quad (2)$$

Kulkarni et al. introduced the multi-rate link metrics that are similar to Eqs. (1) and (2) [5]. In their approach, however, the detailed methodology on estimating the value of multi-rate link metric is not clearly discussed.

The original ETX and ETT rely on broadcast hello exchanges. As pointed out in [6], broadcast transmissions use a fixed and low link rate that may differ from the actual rates for data transmissions. The original measurement approach becomes less accurate, as $|\mathbb{R}|$ increases; for example, in the case of IEEE 802.11n PHY [7], there are 128 possible rates.

We consider a new method for the link quality estimation. As the calculations of d_f and d_b are based on the knowledge of PER (Packet Error Rate) that depends on ℓ and the employed rate (r_i), the estimation of a link metric becomes simple if we have a predetermined PER vs. SNR (Signal-to-Noise Ratio) information in advance. Such a table can be obtained either from the measurement [8] or from the vendor's datasheet [9]. Upon the reception of packets from a neighbor, a node measures the average SNR by measuring both RSSI (Received Signal Strength Indication) and the observed background noise level, and then PER is obtained from the table.

As similar approach, i.e., estimating the PER by looking up a predetermined PER vs. SNR mapping table has been proposed and used for the purpose of a link rate adaptation in the WLAN field; the receiver employs the SNR information to determine the highest throughput modulation and coding scheme, and informs the transmitter via a four-way handshake [10]. We employ an SNR-triggered link rate adaptation scheme in this paper and assume that the mapping table is shared in a cross-layer manner by software blocks that select the link rate at the MAC layer and estimate the link quality metric at the network layer. This setting makes the estimate of a given link metric consistent and prevents the metric value from unexpectedly fluctuating over time. The dynamics of the considered link metric values is not a desired property [1,2], since it may lead the route to frequent, unnecessary changes [11].

We verify the proposed metrics in terms of the accuracy of the link abstraction. We assume that two compared metrics, namely, the legacy and the proposed ones commonly use the PER vs. SNR mapping information for the purpose of a fair comparison. Other components in calculating legacy metrics are the same as the original ones, i.e., ETX uses the size of a hello message for the calculation of the forward and the backward delivery ratios (d_f and d_b) and ETT uses the most frequently used link rate (r) for its calculation. Since we adopt the SNR-triggered rate adaptation for the link rate selection, r should be the result of a link adaptation decision.

Fig. 1 shows the difference between the legacy and the proposed metrics. The x-axis stands for the distance between two nodes, thus reflecting the increased path loss as the distance increases. ETX and ETT are described in red line and dotted blue line, respectively. No difference in ETX is observed by the distance of approximately 31 m; however, an exponential difference is shown if the distance increases longer than that. The best result of an ETX calculation is one, which means that only a single transmission is enough for the successful delivery of a data packet by using the current link rate. While the difference of the two metrics (the legacy ETX and the proposed ETX) is zero, the calculated ETX value is one. From the distance of 31 m, however, ETX calculations get distorted since the difference in PER of data and hello packets is shown in the resultant ETXs.

More significant differences than ETX are shown in ETT several times. The legacy ETT uses the most frequently used link rate (r) in its calculation. However, the proposed one selects r so that the resultant ETT becomes the minimum. This fundamental difference in selecting r is shown in the difference ratio (%) in Fig. 1. Unlike the case of ETX whose difference appears after the distance of 31 m, the legacy and the proposed ETTs never match in the entire range of the node distance. In particular, it is observed that the difference becomes huge where the link rate is about to change. Such an estimation error occurring in each link would affect the final route decision in a cumulative manner since the link metrics are used in such a way as addressed below.

In the case of ETT, a route is set up by selecting the path that has the minimum sum metric among all available paths. The problem to construct the best route with ETT is to find CETT* (Cumulative ETT *):

$$\mathrm{CETT}^* = \underset{j \in \mathbb{P}}{\operatorname{argmin}} \mathrm{CETT}_j, \quad (3)$$

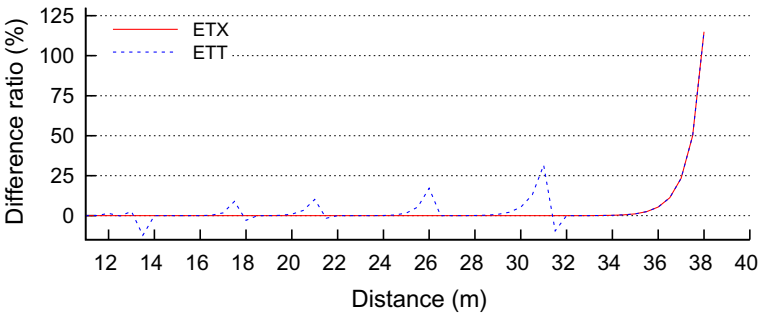

Fig. 1. Estimation error when link metric is calculated by using hello messages.

where $\mathbb{P}$ is the set of all feasible paths from the source to the destination and $CETT_j$ is the summed ETT over a path j, where $j \in \mathbb{P}$.

Since we consider a single-channel/-radio mesh network in this paper, we do not have to utilize WCETT (Weighted Cumulative ETT) [2] that is designed to give priority to the least-congested-channel route in multi-channel/-radio environments.

3. Routing protocols

We revisit routing protocols AODV [4] and OLSR [12], and consider which properties should be carefully utilized and enhanced.

3.1. AODV

3.1.1. Use of link quality metrics

The route discovery of AODV relies on the exchange of RREQ (Route Request) and RREP (Route Reply) packets between the source and the destination. For AODV with HOP, the shortest-hop path is preferred, and hence, there is no need to process and forward later received RREQs with the same broadcast ID unless they have a higher sequence number (i.e., have fresher route information).

With the new link quality metrics, the protocol needs modifications to find the optimal path. Duplicate RREQs that carry a better cumulative link metric value must be forwarded, so that all the possible routes are considered.

To demonstrate the effectiveness of a duplicate RREQ forwarding, we configure an example topology as shown in Fig. 2. N_0 and N_5 are the source and the destination nodes, respectively, and it is assumed that two-hop neighbors of each node are reachable. The feature over each link stands for ETT. The source node with AODV searches the end-to-end path, $N_0 \mapsto N_2 \mapsto N_3 \mapsto N_5$ over which CETT is 4.4 and 0.77 Mbps throughput is achievable. The initial RREQ is received by N_1, N_2, and N_6; therefore, the forwarded RREQs from N_1 and N_6 are filtered out by N_2. Next, the RREQ forwarded by N_2 is received by N_3 and N_4, and then N_3 wins the channel contention, thus forwarding the RREQ that is received by the destination. An RREP generated by the destination finally informs the source node of the decided route. On the other hand, a different route, $N_0 \mapsto N_6 \mapsto N_1 \mapsto N_2 \mapsto N_3 \mapsto N_4 \mapsto N_5$ is searched by the new AODV that allows duplicate RREQ forwarding. The measured CETT over the new route is 1.2 and the achievable throughput is 1.99 Mbps, which is more than twice of the previous result. Note that the proposed approach does not require any new network-wise overhead, but an additional RREQ processing at each intermediate node, which does not typically affect the throughput performance.

3.1.2. Link failure detection

AODV utilizes an RERR packet to alert the link disconnection. The RFC specifies how to detect a link failure as follows: timeout expiration in `HELLO_INTERVAL` × `ALLOWED_HELLO_LOSS` [13]. When a link failure is detected and RERR is triggered, every node that receives the RERR removes the corresponding entry from its routing table and rebroadcasts it. Source nodes that use the broken link bootstrap the route establishment process by sending an RREQ.

As mesh routers are typically stationary, link failures due to mobility are rare. In addition, a link is disconnected and RERR is triggered when a transmission fails due to packet collisions, interference, or inadequate link rate selection, which often occur temporarily. Although the route rediscovery process is crucial to maintain the end-to-end connectivity, unnecessary triggering of route recovery wastes network resources. In the case of TCP (Transmission Control Protocol), a TCP timeout may happen due to a needless RERR packet generation and TCP performance drastically decreases.

To reduce unnecessary RERR triggering cases, we revise the detection procedure algorithm as follows:

Algorithm 1. Revised Link Failure Detection

1. *A mesh node, $\mathcal{A}$ that is expecting the reception of the next hello from its neighbor $\mathcal{B}$, sends a unicast HREQ (Hello Request) to $\mathcal{B}$, before the timeout expiration (e.g., at* `HELLO_INTERVAL` × (`ALLOWED_HELLO_LOSS` − *1)).*
2. *When the HREQ arrives at $\mathcal{B}$, it replies with a unicast HREP (Hello Reply).*
3. *If $\mathcal{A}$ does not receive the HREP, $\mathcal{A}$ generates an RERR as specified in [13]. Otherwise, $\mathcal{A}$ does not invoke the link failure detection and route rediscovery procedure.*

The effectiveness of Algorithm 1 can be evaluated by showing how much TCP performance is affected by the misused RERR generation and how much gain the revised link failure detection algorithm can achieve. We consider a grid topology as shown in Fig. 8 that is composed of 48 nodes and one gateway, with the link distance of 15 m. A randomly selected source node sends a long-lived TCP flow toward the gateway that is located at the right-upper corner. ETX is used in every route selection. A prohibitive RERR generation is easily observed in many cases and we representatively choose two examples here.

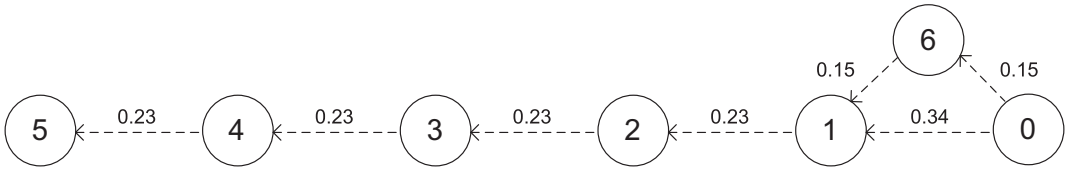

Fig. 2. An illustrative example showing the effectiveness of duplicate RREQ forwarding. The feature over each link stands for ETT.

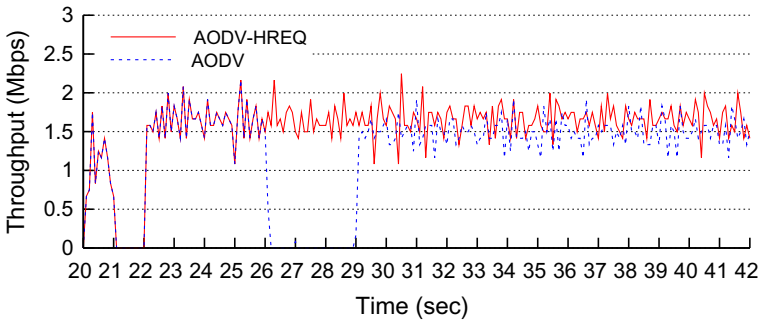

(a) A TCP flow from N_5 to the GW.

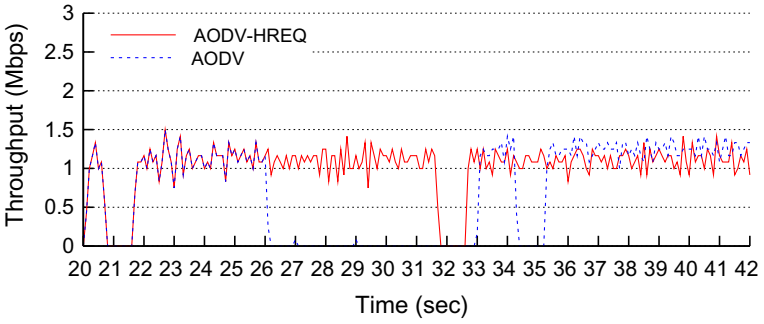

(b) A TCP flow from N_2 to the GW.

Fig. 3. Performance comparison of AODV and AODV with the revised link failure detection.

Fig. 3a and b show end-to-end throughput when N_5 and N_2 generate TCP flows, respectively. The red line shows the throughput of AODV with the revised link failure detection algorithm (AODV-HREQ) and the blue dotted line represents that of the original (AODV). When N_5 starts generating TCP packets at 20 s, AODV on N_5 bootstraps a route construction, thus resulting in the route, $N_5 \mapsto N_{13} \mapsto N_{27} \mapsto N_{41} \mapsto N_{48}$ (GW). After about 1 s elapses, three Duplicated ACKs (3-DUPACK) are received at the TCP source and TCP Tahoe deals with such a 3-DUPACK event as a TCP timeout. Next, the TCP source reduces the congestion window to one MSS (Maximum Segment Size) and holds TCP packets during 1-s TCP timeout interval, which is the default configuration in the ns-2 simulator for congestion avoidance, and is doubled for every continuous timeout event [14]. The problem comes around at 26 s when a TCP ACK packet is collided with Hello packets generated by N_{13}. According to the protocol, N_{13} generates RERR and it is propagated over all routes that include the link. The gateway that has enqueued TCP ACKs, but has no route to the source node starts building a new route. While the gateway node builds a new route, TCP timeout events happen two times in series at the source node; therefore, the source node holds to send TCP packets during 3 s. Finally, the TCP flow resumes at around 29 s over the new route, $N_5 \mapsto N_{20} \mapsto N_{34} \mapsto N_{48}$. On the other hand, AODV-HREQ does not suffer from such an RERR problem and achieves 1.84 Mbps on average, while AODV's throughput is 1.56 Mbps. As observed in Fig. 3a, an RERR generation and a consequent route re-establishment can result in sequential TCP timeout events by which the TCP timeout interval multiplicatively increases. In the case of N_2 that initially has the route, $N_2 \mapsto N_4 \mapsto N_{19} \mapsto N_{34} \mapsto N_{48}$, an RERR is generated by N_4 at around 26 s and again the gateway initiates re-constructing a route to the source node. In this case, unfortunately, the route re-construction takes longer time than 3 s, and hence, the TCP timeout interval increases up to 4 s, i.e., the TCP flow does not resume for 7 s (from 26 to 33 s). Consequently, the average throughput performance of AODV and AODV-HREQ are 0.97 and 1.25, respectively. In summary, AODV-HREQ achieves 18% and 29% gain of TCP throughput over AODV in the cases of N_5 and N_2, respectively, and this shows the effectiveness of the proposed algorithm for the link failure detection.

3.1.3. Receiver-centric metric caching

When a route is being established, RREQs need to convey link metrics that will be used for the route decision at the destination. Hence, each node must include the link metric information to all its neighbors in the RREQ before forwarding, as it does not know which neighbor will be the next hop node of the route.

This approach drastically increases the size of RREQ messages as the number of neighbor nodes increases, which contributes to the overhead of the route setup. Let's assume that a link quality can be presented in a *double* variable whose standard size is 8 bytes. To attach one link metric toward a neighbor specified by an IP address, 12 bytes are required. The amount of the increased size of each

RREQ is determined by the node density in a two-dimensional area and the communication range of each node. Table 1 shows how many bytes are additionally required to inform the neighbors of the one-hop link quality information. In the case that the communication range is 100 m (D = 100 m) and the node density is 0.0001 m^{-2} (i.e., one node in $100 \times 100\ m^2$), 38 bytes are added to every RREQ. However, the additional amount increases proportionally to the node density and thus 3770 bytes are required when the density is 0.01 m^{-2}. As for an enterprise network, a shorter value of D and a higher value of the node density is likely to be reasonable. If D is set to 20 m and 0.01 m^{-2} node density is assumed, the additional increment becomes 151 bytes for every RREQ transmission.

In our scheme, instead of making an RREQ sender include metrics of all one-hop links and deliver them to all neighboring nodes, the metric of a link is appended in the RREQ by the receiver of the link (i.e., the node that just received the RREQ). Accordingly, no addition in the RREQ size is required based on the proposed method for the link metric caching and forwarding, which results in a huge overhead reduction in the network-wise viewpoint. Let $\mathcal{A}$ and $\mathcal{B}$ be adjacent neighbors. According to the typical hello-based quality estimation [1,2], $\mathcal{B}$ measures the link quality in terms of the metric of interest, say $LQ_{\overline{\mathcal{AB}}}$. Instead of transferring $LQ_{\overline{\mathcal{AB}}}$ to $\mathcal{A}$, $\mathcal{B}$ keeps and uses it for the future RREQ forwarding. As a result, $\mathcal{A}$ does not have to include metric value of all neighboring links in an RREQ.

3.2. OLSR

3.2.1. Routing entry calculation

In OLSR, each node maintains the neighbor and topology tables by receiving and processing hello and TC (Topology Control) messages, respectively. A node runs the shortest path selection algorithm, whenever any of the following conditions is satisfied: (1) a hello or TC message that conveys new link information is received, (2) a link is detected as not a *bi-directional* link (during a predetermined time interval, hellos have not been exchanged successfully in both directions), and (3) a route to any destination expires.

The shortest path calculation described in OLSR [4,15] optimally works with HOP; starting from 1-hop neighbors, the source node chooses its MPR as the first hop node, and then the next hop is chosen among MPRs of the first hop node. This operation is repeated until reaching the MPR of the destination. This algorithm is the same as the Dijkstra's algorithm in the sense that a route is determined by the minimum hop count metric and all intermediate nodes are MPRs. To use non-binary link quality metrics, we modify the routing entry calculation as follows: when the source or an intermediate node selects the next hop, it follows the Dijkstra's algorithm in terms of ETX/ETT and considers all reachable 1-hop neighbors as the candidate. Since it is obvious that the existing routing entry calculation is likely to yield a non-optimal route, we omit the evaluation of the proposed improvement.

Table 1
The amount of increased size of RREQ.

Density (#/m^2)	D = 100 m (bytes)	D = 50 m (bytes)	D = 20 m (bytes)
0.0001	38	10	16
0.001	377	95	76
0.01	3770	943	151

3.2.2. MPR selection

The concept of MPR (Multi-Point Relay) is a core in OLSR that contributes to the optimization of the routing process. In order to reduce the overhead in disseminating link quality information, each node selectively chooses its MPRs. An MPR node is responsible for forwarding link information between itself and its MPR selectors, i.e., the ones who select the node as their MPR.

As the amount of disseminated information directly hinges on the number of MPRs selected by each OLSR node, the MPR selection rule is the critical part of the OLSR design. The selection criterion is as follows: $\mathbb{M}^* = \text{argmin}_{\mathbb{M}\subset\mathbb{N}_1}|\mathbb{M}|$, such that $\mathbb{M}$ covers $^{\forall}n$ for $n \in \mathbb{N}_2$, where $|\cdot|$ is the operator that counts the number of elements in a given set, $\mathbb{M}$ is the set of MPRs chosen by the MPR selector node $\mathcal{A}$, and $\mathbb{N}_i$ is the set of $\mathcal{A}$'s i-hop nodes.

With respect to non-binary link metrics, the MPR concept itself might throttle the optimization of OLSR route establishment, even if it reduces the overhead. Fig. 4 shows an example of this problem. The network is composed of five mesh nodes and the average employed link rates are shown in the unit of Mbps. Small square boxes near each mesh node are the selected MPRs that cover all two-hop neighbors of the reference node. Because N_4 chooses N_2 as its MPR, the link quality information between the two nodes, $LQ_{\overline{24}}$ is propagated over the network conveyed into hellos and TCs generated by N_2. In this example, the link information between N_3 and N_4, i.e., $LQ_{\overline{34}}$ never reaches N_0 because of the MPR selection by N_4. Hence, N_0 has no way of knowing $LQ_{\overline{34}}$.

3.3. Offline optimal routing (MANUAL)

We build a reference routing model called MANUAL that provides the optimal route in terms of a given link metric; before starting any active data session, each mesh node collects all required link metric information and runs the Dijkstra's algorithm to find the optimal route toward all destination nodes. Then, a source node compares the end-to-end metrics (e.g., sum metrics in this paper) and selects the optimal path that presents the best end-to-end metric. Note that there could exist multiple optimal paths. This routing protocol shows the performance upper bound in terms of a given link quality metric and helps us understand the underlying causes that degrade the throughput of the considered routing strategies, i.e., all possible combinations of AODV/OLSR and ETX/ETT.

4. Evaluation framework

To comparatively evaluate the effect of various combinations of link metrics and routing protocols on the

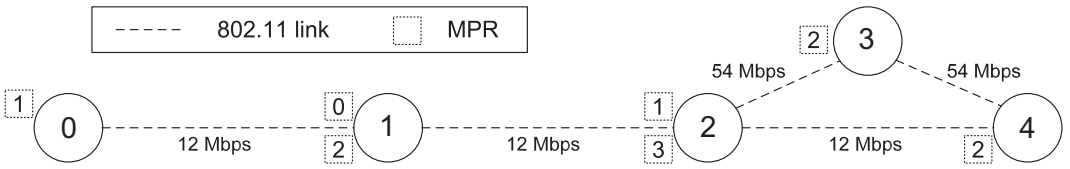

Fig. 4. An illustrative example of the MPR selection problem.

performance of wireless mesh networks, we modify the ns-2 simulator. AODV [14] and OLSR [16] are modified to support ETX and ETT. In order to observe the optimal route setup and its end-to-end performance, an offline route calculation is executed with MANUAL before activating traffic. Single-channel, single-radio environment is considered during all evaluations.

IEEE 802.11 module is enhanced to support 802.11a PHY. For the link rate selection, we use the RTS (Request-To-Send)/CTS (Clear-To-Send)-based SNR-triggered link rate adaptation scheme [10]. Accordingly, the RTS/CTS exchange is enabled by default during simulation runs. This makes the analysis of routing performance clear as over/underestimated link rates are suppressed. Hidden nodes can easily exist in multi-hop wireless networks. Therefore, we force mesh nodes to transmit all control frames at the lowest transmission rate to minimize the hidden node effect.

We assume that a mesh access point forwards traffic from or to client devices, thus working as a source or a destination node of such traffic. Each mesh node transmits with 20 dBm transmission power and all nodes are stationary. The background noise level is set to −93 dBm. We use a log-distance path-loss model with the path-loss exponent of four [17] in AWGN (Additive White Gaussian Noise) channel to simulate an indoor mesh environment. As observed in [18], CS (Carrier Sense) range of the 802.11a PHY is completely covered by the RTS/CTS transmission range. We hence set the CS range to the same range of the RTS/CTS transmission (approximately 39.5 m).

We conduct simulation runs under various mesh topologies. We use LLC/IP/TCP (IEEE 802.2 Logical Link Control/Internet Protocol/Transmission Control Protocol) as the upper layer protocol suite. Long-lived TCP flows are used and the MAC payload size is fixed at 1024 bytes.

In our simulation model, each mesh node calculates the considered link metrics between itself and its neighbors based on distances and the given path-loss model, which is a ground reflection (two-ray) model [17]. We run multiple simulations (up to 30 times) with different random seeds for a given network topology. In case that the detailed protocol operation needs to be observed and analyzed, single-run-based evaluation results are presented (Section 5), while the averaged view of network performance is shown in case that the qualitative analysis is required (Section 6).

5. The effect of route optimality

In this section, we investigate the effect of route optimality on the end-to-end throughput performance, for a single flow without any interflow interference.

5.1. Non-optimal path: unforeseen protocol behavior

We first consider multi-hop chain topologies, with varying link distance r in meters ($1 \leqslant r \leqslant 21$) between adjacent mesh nodes. A chain topology is composed of seven mesh nodes, where two end nodes work as the source and the destination. Fig. 5a and b plot simulation results for end-to-end throughput and the differences between ETX and ETT sum metrics and the optimal. The throughput decreases in general as r increases for any routing strategy. We also observe throughput reductions at specific r values.

At $r = 19$ of Fig. 5a and b, AODV and OLSR show the same sum metric for both ETX and ETT that is the worst out of the entire range of r. It should be noted that in this topology, the optimal route is to forward packets to the next adjacent node achieving the minimum sum metric. We observe that the throughput performances of AODV and OLSR are not the same as shown in throughput graphs. Fig. 6 illustrates the established end-to-end paths between N_0 (source) and N_6 (destination), and RTs (routing tables) for specific nodes, when $r = 19$.

First, in Fig. 6a, we look into the case of OLSR with ETX. On the left side of each node, the selected MPRs are shown inside rectangles. The MPR selection criterion used in our simulations follows the original implementation [16]. The one-hop neighbor set of N_0 includes N_1 and N_2, since the CS range is set to 39.5 m. The longest-distance link (e.g., the link between N_0 and N_2) shows the link quality of 3.76 in ETX, which means that on average 3.76 times transmission attempts are required for a successful packet delivery. We observe that the link information of the following four links is not disseminated over the network due to the MPR selection as addressed in Section 3.2.2: $ETX_{\overline{12}}$, $ETX_{\overline{23}}$, $ETX_{\overline{45}}$, and $ETX_{\overline{56}}$. Accordingly, the source would not obtain the information of links between N_4 and N_5, and between N_5 and N_6, thus having $CETX_{\overline{06}} = 7.76$. On the other hand, N_3 is able to receive a hello from N_5, in which the link information of all one-hop neighbors of N_5 is conveyed. Hence, N_3 has the optimal route toward N_6 in contrast to N_0. As a result, the throughput performance of OLSR reaches that of MANUAL, which could not be expected by the source whose forecast of the route is supposed to be $N_0 \mapsto N_1 \mapsto N_2 \mapsto N_3 \mapsto N_4 \mapsto N_6$. A similar phenomenon is repeated for the reverse direction as the link information of $ETX_{\overline{12}}$ and $ETX_{\overline{23}}$ is not propagated to N_6. Note that such a non-optimal route construction happens with ETT as well. We believe that although the MPR of OLSR reduces control overhead, it leads to poor route selection when used with non-binary link metrics.

In fact, OLSR shows a near-to-MANUAL performance over the entire range of r with both ETX and ETT, despite

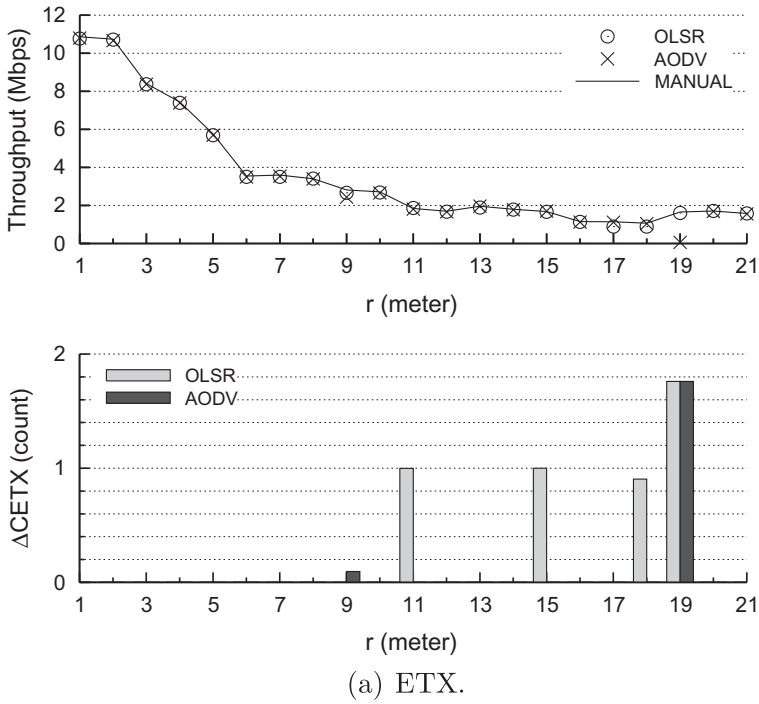

(a) ETX.

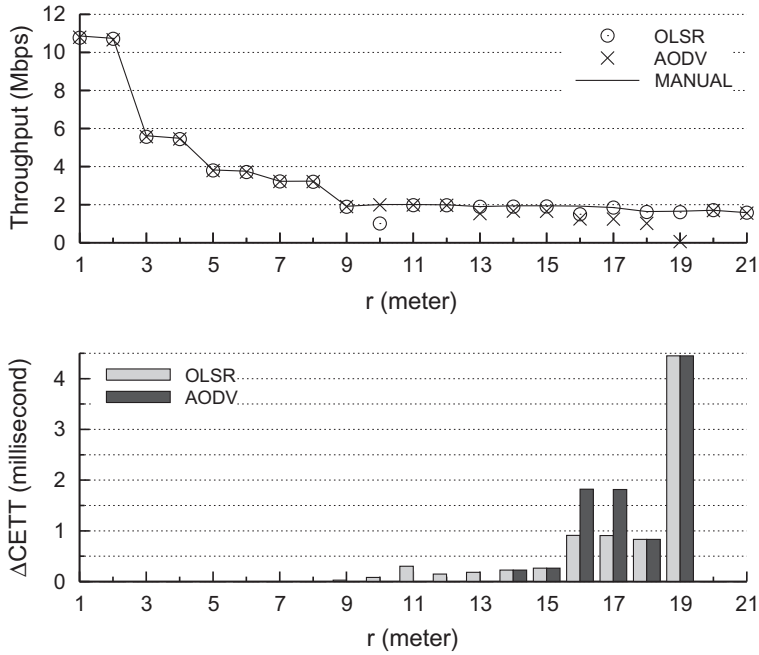

(b) ETT.

Fig. 5. Performance comparison of MANUAL, AODV, and OLSR in chain topologies with ETX and ETT metrics.

a few cases of metric differences. This can be explained with the same reason as the previous case ($r = 19$). With the chain topology, only when $r = 16$ with ETT, OLSR shows degraded performance due to poor MPR selection. In other words, even if the expected route construction from the source's point of view is non-optimal, the actual trajectory of packets often match up to the optimal route. This results from the feature of link state routing. Note that in a few cases, OLSR does not work as well as MANUAL even though the sum metric indicates the optimal route setup, e.g.,

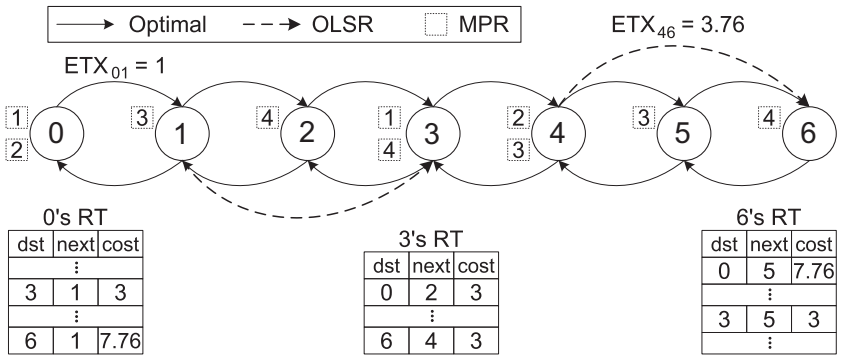

(a) OLSR.

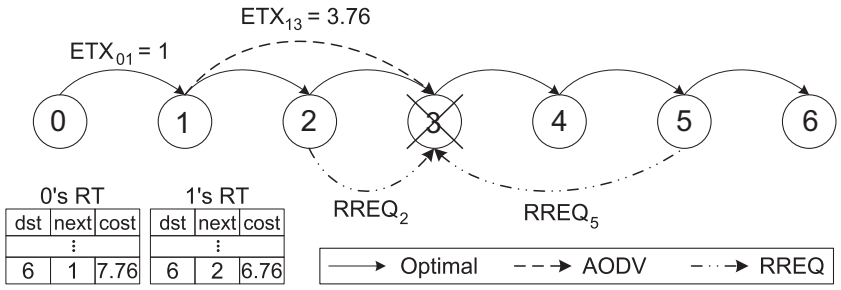

(b) AODV.

Fig. 6. Non-optimal route setups with ETX in a chain topology where $r = 19$.

$r = 10$ in Fig. 5b. It is due to an unexpected TCP timeout, which results from multiple packet collisions and a timer expiration with a missed TCP ACK.

Now, let's take a look at AODV case in Fig. 6b. We observe that the RREQ initiated by the source is forwarded by intermediate nodes with the following sequence: $N_0 \mapsto N_1 \mapsto N_3 \mapsto N_2 \& N_5 \mapsto N_4 \mapsto N_6$. Since N_3 forwards the RREQ ahead of N_2 in this case, N_4 and/or N_5 possibly initiates an RREQ forwarding before N_2 does. When N_2 and N_5 transmit their RREQs simultaneously, a collision happens; hence, N_3 does not receive the link metric between N_2 and N_3. As N_3 does not include the link information between N_2 and N_3 in its RREQ, the source eventually sets up an end-to-end route without such information. This leads to a degraded performance shown in Fig. 5a and b at $r = 19$.

Similar results are obtained whenever ΔCETX or ΔCETT shows a non-zero value in Fig. 5a and b. Since such an event results from the hidden interferers, it will also occur with non-uniform chain cases where hidden nodes exist. Consequently, we argue that the non-optimal route setup with AODV leads to throughput degradation, whereas it is not always straightforward with OLSR due to its link state feature.

5.2. Impact of link metric design on end-to-end throughput

We compare the impact of link metrics on the multihop performance. Fig. 7 shows the throughput and the hop count with ETX and ETT. MANUAL routing protocol is used in this comparison. The hop count graph shows that ETX prefers the shortest-hop path, while ETT gives a higher priority to the faster link. ETT overtakes ETX throughput when $r = 11$. ETX shows high-throughput when the destination is reachable within two hops from the source; otherwise, ETT shows better performance when $r \geqslant 11$.

5.3. Sensitivity of route construction to background traffic

We now investigate the impact of route optimality on the route construction when background traffic exists. We consider a grid topology as shown in Fig. 8 that is composed of 48 nodes and one gateway, with the link distance of 15 m. The interfering background traffic is generated from N_{44} (INT. SRC) to N_{20} (INT. DST), while one of 47 nodes (except N_{44}) is selected as a source and activates a long-lived TCP flow towards the gateway. 1000-byte CBR flow with 5 Mbps generation rate starts to create interference for 3 s when the TCP flow is initiated.

Figs. 9a and b, and 10 show the comparison of throughput of different routing strategies, metric differences, and hop counts. Results are sorted by mesh node indexes (x-axis) that match up to those in Fig. 8. We learn from this experiment: (1) Non-optimal route setup due to interference leads to throughput decrease; (2) AODV shows different (lower in general, yet sometimes higher) throughput compared with MANUAL; (3) TCP timeout results in performance degradation in the case of OLSR with ETX; and (4) ETT finds higher throughput routes than ETX.

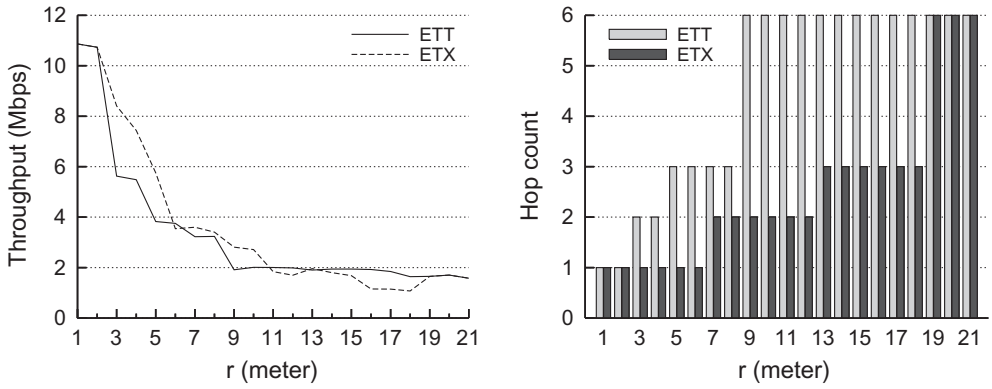

Fig. 7. Performance comparison of ETX and ETT with MANUAL.

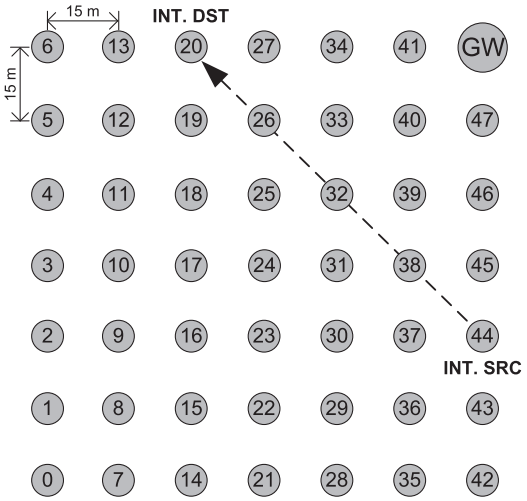

Fig. 8. A 7 × 7 square-grid topology network. N_{44} generates an interfering signal that is destined to N_{20}, whereas one out of 47 (except N_{44}) mesh nodes activates a TCP session destined to the gateway.

5.3.1. Non-optimal sum metric yields throughput degradation

We observe that non-optimal route setup results in degraded throughput performance in most cases. In the case of OLSR with ETT, the optimal route is not used for about 70.8% cases out of which about 91% cases generate less throughput than that of MANUAL. Compared with the previous chain-topology cases, the ratio of non-optimal routes to optimal ones increases with nodes in a lattice shape. The two-dimensional node deployment makes more number of reachable links than those in the chain cases, while selected MPRs do not disseminate all such link information (ETT) throughout the network. Therefore, the number of links whose link metric values are not informed to other nodes increases in the grid topology, which contributes to non-optimal route construction and degraded throughput performance. We expect if the number of available links increases in a specific node deployment (e.g., a 3-dimensional building structure), non-optimal route construction happens more frequently. The case of OLSR with ETX is discussed in detail later.

Three cases that build non-optimal paths, i.e., N_0, N_6, and N_{20}, show similar performance to MANUAL. As observed in Section 5.1, an intermediate node can find the optimal route although the source node has non-optimal route information. It originates in the feature of link state routing and happens when the intermediate node successfully receives hellos or TCs, while the source does not.

Not only the non-optimal setup, but another aspects also contribute to the throughput degradation. First, the constructed route has the same CETT with the optimal route made by MANUAL, yet the actual packet trajectories defer, thus yielding degraded throughput performance. We observe that the four cases of N_{26}, N_{39}, N_{45}, and N_{46} show the identical sum metric to that of MANUAL. However, they use different paths when sending TCP packets. As a source node can find multiple feasible paths, it is possible to have more than one path that have the identical and optimal sum metric. Therefore, such four cases are exceptional, yet possible scenarios, showing the optimal sum metric, but non-optimal throughput. Second, there are other two noticeable cases such as N_{36} and N_{47}, where the dominant cause that yields throughput degradation is not the non-optimal route setup, but the TCP timeout. Due to interference, TCP timeout occurs, leading to degraded throughput. Other than those exceptions, the cases that have the identical sum metric show throughput performances as good as those of MANUAL (with 10% error margin).

5.3.2. AODV sometimes generates higher throughput than MANUAL

AODV performs better than MANUAL in eight cases as shown in Fig. 9a. Such an interesting behavior of AODV happens in the cases of N_4, N_5, N_{12}, N_{21}, N_{22}, N_{23}, N_{24}, and N_{28}, where AODV+ETX does not provide the optimal route due to the losses of control packets. This means that the ETX-based route construction cannot always yield the highest throughput performance due to the inaccurate link metric design of ETX (i.e., in [1], ETX originally assumes the single transmission rate and homogeneous data packet size).

5.3.3. TCP timeout can degrade performance of OLSR with ETX

Table 2 shows the percentage of average throughput degradation of OLSR and AODV compared with MANUAL.

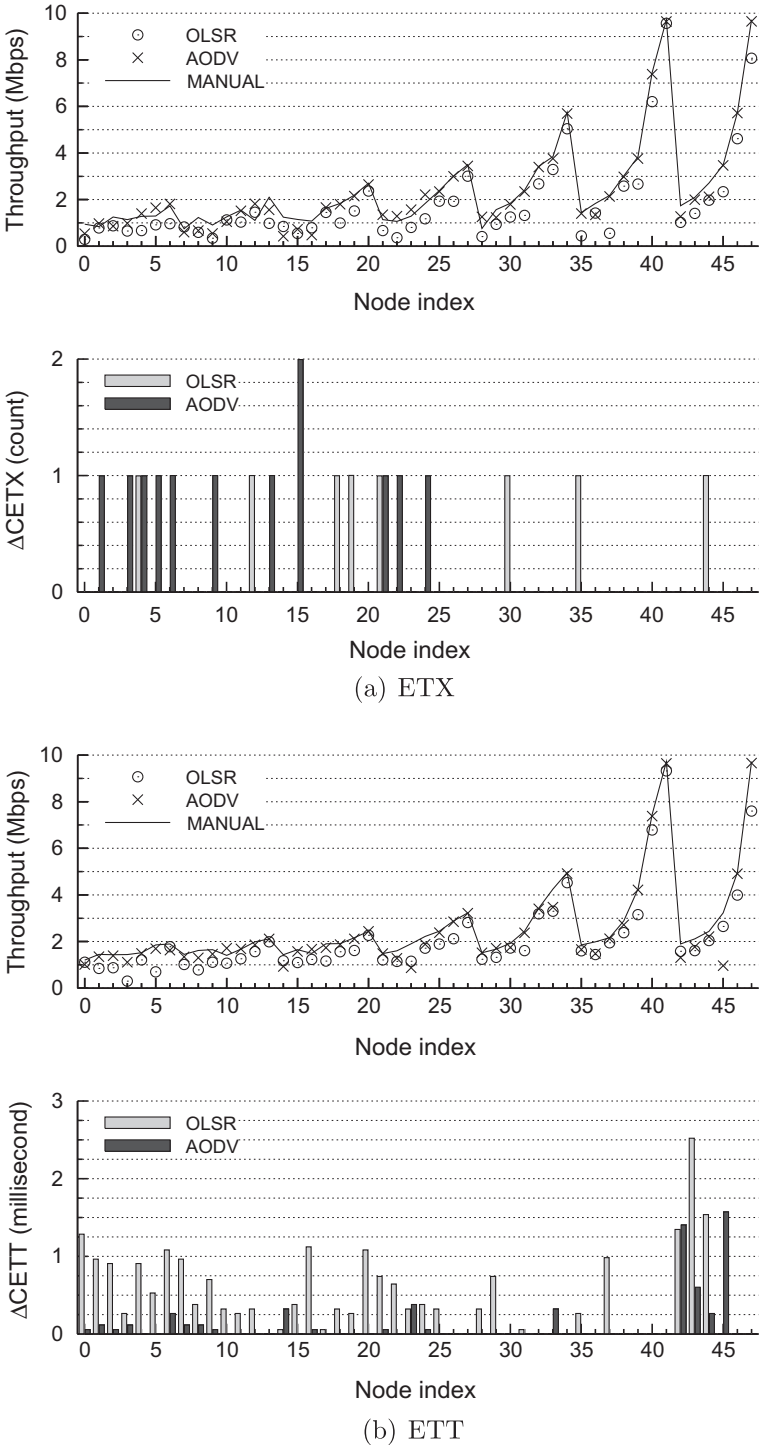

Fig. 9. Performance comparison of MANUAL, AODV, and OLSR in grid topologies with ETX and ETT metrics.

OLSR shows larger throughput degradation than AODV, especially with ETX. Metric difference shows that OLSR generates non-optimal routes in eight cases, when working with ETX. We take into account the impact of TCP timeout with OLSR. With OLSR, TCP times out 44% more often with ETX than ETT.

As illustrated in Fig. 10, ETX-based routing that selects the minimum CETX route prefers the shortest-hop path, which in turn makes the length of each hop long. Thus, a low transmission rate is likely to be used, which requires a long transmission time. If a hidden interferer exists, where node $\mathcal{C}$ receives nothing, while nodes $\mathcal{A}$ and $\mathcal{B}$

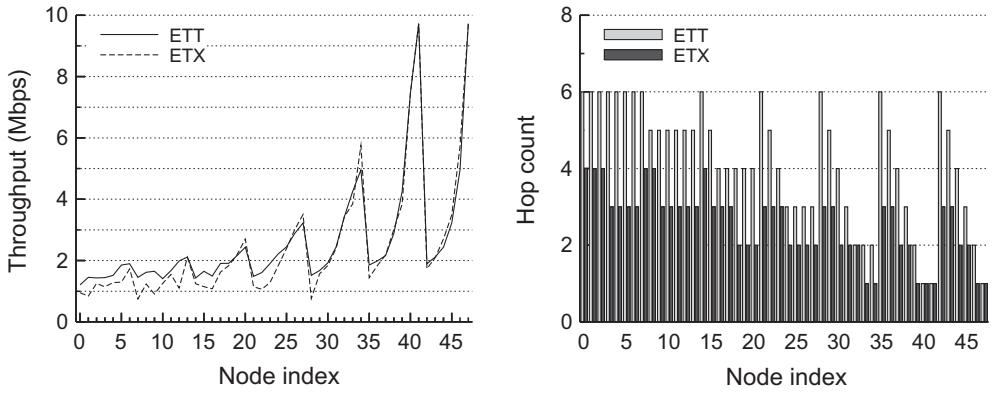

Fig. 10. Comparison of ETX and ETT along with MANUAL.

Table 2
Throughput reduction with of OLSR and AODV.

Metric	AODV (%)	OLSR (%)
ETX	5.3	31.4
ETT	9.0	23.4

exchange RTS and CTS, an ETX-based path is more susceptible to hidden interference (e.g., from C) than a path based on ETT due to the long packet transmission time. With OLSR, ETX had more collisions due to hidden interference than ETT in 29 out of 48 cases. This result contradicts our expectation of ETT generating more collisions as it builds routes with longer hops than ETX.

The reason why AODV is less affected by the interfering flow than OLSR is the exposed time duration of routing control packets to interference. While the average required time for an RREQ/RREP exchange is 1 s in grid scenarios, OLSR's control packets such as hellos and TCs are affected during the entire interference duration, i.e., 3 s. In other words, as the chance that each node cannot maintain accurate link state information due to the interfered control packets increases, the expected network performance via a constructed route decreases. That is the reason why AODV shows better performance than OLSR.

5.3.4. Impact of link metric design on end-to-end performance

Fig. 10 shows throughput performance and corresponding hop counts, when a selected source node operates MANUAL routing. The collected data is sorted with respect to the hop count of ETT-based routes. The hop count graph indicates that ETX prefers the shortest-hop path, while ETT gives higher priority to the faster link. ETX shows high-throughput when the destination is reachable within two hops from the source. In other cases, ETT shows the better performance (on average 11.9% throughput gain over ETX).

6. Interplay of route optimality and interflow interference

Finally, we investigate the interplay of route optimality and interflow interference when multiple concurrent flows exist. The same grid topology in Fig. 8 is considered. There are k (=2, 4, and 8) concurrent TCP flows with randomly selected non-duplicate sources out of 48 mesh nodes. We repeated the experiment using 30 different random seeds to present the averaged results.

We here consider the routing strategy of OLSR with ETX[1] to observe the impact of both route optimality and interflow interference on throughput performance, and their interaction by comparing the measured metric difference and JFI (Jain's Fairness Index) [19]. We use a normalized JFI (nJFI) to make the lowest value zero for any k. That is, $\text{nJFI} = (\text{JFI} - \frac{1}{k}) \times \frac{k}{k-1}$.

Fig. 11a shows the measured end-to-end throughput of MANUAL (x-axis) and OLSR (y-axis). The average aggregate throughput values of MANUAL over 30 random seeds are 2.96, 3.77, and 4.97 Mbps, for $k = 2$, 4, and 8 (depicted as k SRCs in the graphs), respectively. Meanwhile, the portion of paths that return the optimal sum metric value becomes smaller as the number of k increases as shown in Fig. 11b. This is basically due to the same reason as addressed in the previous subsection, i.e., as the chance that a node cannot maintain accurate link information due to the interfered control packets increases, the expected network performance via a constructed route decreases in a link state routing protocol.

When multiple concurrent flows exist, there could be unfair bandwidth sharing since neither TCP nor the 802.11 MAC provides fair resource allocation. Hence, a few sources may dominate the network resources. It was shown in [20] that high aggregate throughput can be achieved at the expense of severe unfairness. We present JFI for different k values in Fig. 11c, where the x-axis is JFI and the y-axis is the cumulative fraction of fairness index. When $k = 2$, the percentage that OLSR constructs the optimal route reaches 85%, while the number of cases that the throughput of OLSR is smaller than that of MANUAL is

[1] As for other routing strategies, we have similar observations when having up to 8 TCP sources. As the number of source nodes increases, however, the JFI drastically decreases, and it is not fairly possible to have the reasonable analysis of throughput performance using the route optimality and JFI information.

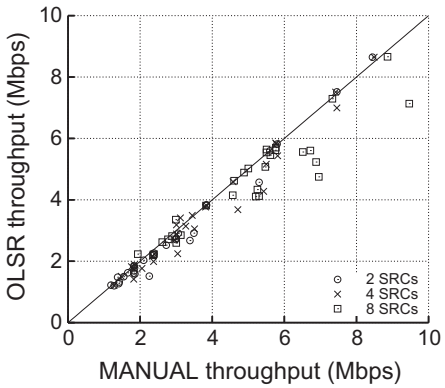

(a) Scatter plot of 90 random scenarios varying the number of source nodes.

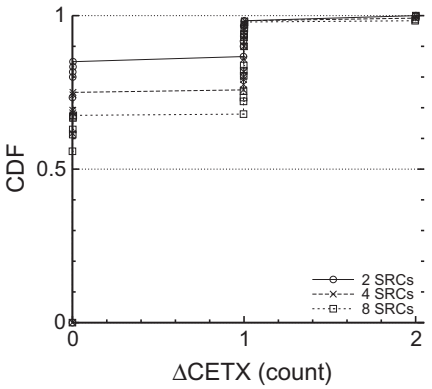

(b) Cumulative fraction of metric discrepancy measured by each source node.

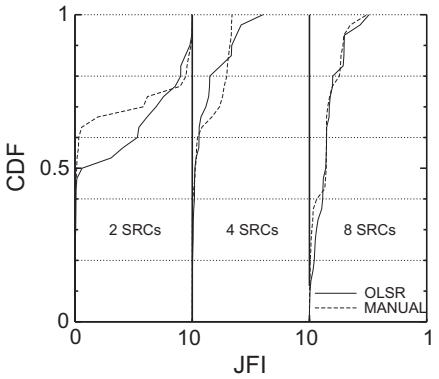

(c) Comparison of cumulative fractions of fairness index for a given number of source nodes.

Fig. 11. Performance comparison of MANUAL and OLSR with ETX when multiple concurrent flows exist in a 7 × 7 square-grid topology.

10 out of 30 (>15%) as shown in Fig. 11a. The fact that MANUAL shows worse JFI in Fig. 11c, explains that its aggregate throughput is higher than that of OLSR.

Except when $k = 2$, MANUAL and OLSR show similar JFI performances. This result indicates that the unfairness itself cannot explain relatively good performance shown in Fig. 11a because both MANUAL and OLSR show similar JFI when $k = 4$ and 8. Meanwhile, the metric difference becomes worse as k increases as shown in Fig. 11b. This is also explained by the fact that the gain of MANUAL over OLSR increases from 6.8% to 8.9%, when k increases from 4 to 8 as presented in Table 3.

We observe that OLSR outperforms MANUAL only in seven cases out of 90. Among them, four cases are due to extremely unfair bandwidth sharing. For other three cases where JFI is high, meaning quite fair, OLSR finds non-optimal routes, yet those routes yield better throughput due to unequal knowledge of link metric among nodes. It is similar to the case in the previous section where ETX fails to find the best throughput path, but its sum metric shows the optimal.

In summary, we conclude that the route optimality is an indicator to predict the end-to-end throughput performance when multiple flows exist. However, an extremely unfair bandwidth share makes such an analysis less meaningful as one or few nodes devour the entire network bandwidth, irrespective of established optimal routes.

Table 3
Aggregate throughput gain of MANUAL over OLSR.

k	2	4	8
Gain (%)	7.2	6.8	8.9

7. Related work

Routing is an important component in achieving high-throughput wireless mesh networks. Designing a link metric that represents the link quality and a routing protocol that selects the best end-to-end path is critical. While a number of link metrics have been proposed to enhance

the routing effectiveness in wireless mesh networks [1,2,21,11,6], little attention has been made to the combinatorial effect of a specific metric and routing protocol pair.

DSDV (Destination-Sequenced Distance Vector) and DSR (Dynamic Source Routing) were revised to utilize ETX in [1]. The effectiveness of ETX was studied by considering various aspects such as routing protocols, link metrics, and different wireless medium environments. There have been many advanced link metrics proposed afterwards.

AODV-ST (Spanning Tree) [22] combines AODV with the spanning tree algorithm to operate in wireless mesh backbone. The relation and cross-impact between the proposed routing protocol and the considered link metrics, HOP and ETT need to be analyzed more thoroughly to more clearly understand the advantage of AODV-ST. The dynamics of ETX and ETT metrics were studied in two field-testing wireless mesh backbones [11]. It revealed that various environmental changes affect the estimates of such metrics and suggested to have a filtering method to make a prudent decision before using the measured metric values. Despite the interesting findings, there is no examination of the impact of routing algorithms on network performance.

IEEE 802.11s standardization group has shown a vigorous activity to standardize a WLAN-based mesh technology for small-to-large-scale regional area [3]. A hybrid scheme of using AODV and an optional tree-based routing is proposed to support a wide range of application scenarios. The 802.11s tree-based routing mainly intends for all mesh nodes to be reachable the root node, which is typically the gateway node. The core operations of the considered routing protocol however are pretty identical to the original AODV. In addition, the draft itself does not include detailed analysis of the expected performances and their internal causes.

Recently, an efficient concept for multi-hop mesh routing called opportunistic routing has been introduced in the literature [23,24]. It has been however, revealed that a great performance gain is achieved by using opportunistic routing when operating with multicast traffic and its contribution to unicast traffic is relatively small.

Miskovic and Knightly investigates an insufficient distribution of the routing information in AODV [25]. The authors address that the routing selection in AODV inherently yields inferior route selections due to overhead reduction actions and a resultant insufficient distribution of the routing information. To mitigate this problem, Miskovic and Knightly propose that wireless mesh networks operating a distance vector routing should have three new features. First, the network needs to be aware of the *historic ranking principle*; nodes maintain historic routing information that is the collection of paths to each destination and their related metric costs reported during all prior route discoveries where the node participated. The collected historic ranking information is smoothed by an averaging filter and consequently, a failure to receive reports from likely optimal paths can be filtered out. Second, each node over the network operates a historically-assisted DETER primitive: relying on the historic ranking, the mechanism adaptively delays forwarding of route-discovery reports until a node receives reports from its best-ranked next-hops for a given destination. Third, each node operates a historically-assisted RESCUE primitive, which is opportunistically activated by neighboring nodes to offer better paths to the node exposed to a potentially inferior route selection. We in this paper focus on the same issue that the DETER primitive is designed to solve: AODV nodes do not process and forward later received RREQs with the same broadcast ID unless they have a fresher route information for the purpose of the overhead reduction. We propose a simple but effective solution, i.e., letting AODV nodes process and forward later received RREQs despite having the same broadcast ID and the same sequence number as presented in Section 3.1.1.

8. Conclusion

This paper analyzes the performance of wireless mesh networks with respect to the route optimality for a given link quality metric. We first propose the improvements to the mesh link metrics to better represent the multi-rate wireless link quality. Several important modifications to the routing algorithms are then considered to operate better in wireless mesh networks. We also present a reference routing model that searches for the optimal route in terms of a given link metric. Comparative study in various mesh environments analyzes the impact of route optimality, link metrics and routing algorithms, on the multi-hop mesh network performance and fairness. We conclude that unexpected protocol behavior and inaccurate design of link metric cause non-optimal route construction based on which the end-to-end performance is degraded. Interference generated by background traffic or from other sources can disturb the optimal route construction, thus making the resultant performance even worse. Accordingly, there is a need to design robust protocol operation and accurate link quality metric that are able to be unaffected by interference, thus building the optimal route in a robust manner. These are important research problems that this paper highlights. Finally, our study provides hints that can be potentially used to devise advanced link metric and routing protocol, and to materialize the optimized network operation for a real wireless mesh network.

Acknowledgement

This research was supported by the MKE(The Ministry of Knowledge Economy), Korea, under the ITRC(Information Technology Research Center) support program supervised by the NIPA(National IT Industry Promotion Agency) (NIPA-2011-(C1090-1111-0004)).

References

[1] D.S.J. De Couto, D. Auayo, J. Bicket, R. Morris, A high-throughput path metric for multi-hop wireless networks, in: Proceedings of ACM MobiCom'03, San Diego, CA, USA, 2003, pp. 134–146.
[2] R. Draves, J. Padhye, B. Zill, Routing in multi-radio, multi-hop wireless mesh networks, in: Proceedings of ACM MobiCom'04, Philadelphia, PA, USA, 2004, pp. 114–128.
[3] IEEE Std., IEEE 802.11s/D4.0, Part 11: Wireless LAN Medium Access Control (MAC) and Physical Layer (PHY) specifications: Mesh Networking, September 2009.

[4] C.E. Perkins, E.M. Belding-Royer, Ad hoc on-demand distance vector routing, in: Proceedings of IEEE WMCSA'99, New Orleans, LA, 1999.
[5] G. Kulkarni, A. Nandan, M. Gerla, M. Srivastava, A radio aware routing protocol for wireless mesh networks, Tech. rep. tr-ucla-nesl-200503-12, UCLA, Los Angeles, CA, USA, March 2005.
[6] K.-H. Kim, K.G. Shin, On accurate measurement of link quality in multi-hop wireless mesh networks, in: Proceedings of ACM MobiCom'06, Los Angeles, CA, USA, 2006, pp. 38–49.
[7] Draft Supplement to IEEE, IEEE 802.11n/D7.0, Part 11: Wireless LAN Medium Access Control (MAC) and Physical Layer (PHY) specifications: Enhancements for Higher Throughput, September 2008.
[8] L. Verma, S. Kim, S. Choi, S.-J. Lee, Reliable, low overhead link quality estimation for 802.11 wireless mesh networks, in: Proceedings of IEEE WiMesh'08, San Francisco, CA, USA, 2008.
[9] Intersil, HFA3861B; direct sequence spread spectrum baseband processor, January 2000.
[10] G. Holland, N. Vaidya, P. Bahl, A rate-adaptive mac protocol for multi-hop wireless networks, in: Proceedings of ACM MobiCom'01, Rome, Italy, 2001, pp. 236–251.
[11] S.M. Das, H. Pucha, K. Papagiannaki, Y.C. Hu, Studying wireless routing link metric dynamics, in: Proceedings of ACM SIGCOMM IMC'07, San Diego, CA, USA, 2007, pp. 327–332.
[12] P. Jacquet, T. Clausen, A. Laouiti, A. Qayyum, L. Viennot, Optimized link state routing protocol for ad hoc networks, in: Proceedings of IEEE INMIC'01, Lahore, Pakistan, 2001.
[13] C.E. Perkins, E.M. Belding-Royer, S.R. Das, Ad hoc on-demand distance vector routing, in: IETF RFC 3561, July 2003.
[14] The Network Simulator – *ns*-2, <http://www.isi.edu/nsnam/ns/>.
[15] T. Clausen, P. Jacquet, Optimized link state routing protocol for ad hoc networks, in: IETF RFC 3626, October 2003.
[16] OLSR ns-2 distribution at MASIUM – <http://masimum.dif.um.es/>.
[17] T.S. Rappaport, Wireless Communications: Principle and Practice, second ed., Prentice-Hall, 2002.
[18] D. Qiao, S. Choi, A. Jain, K.G. Shin, MiSer: an optimal low-energy ttransmission strategy for IEEE 802.11a/h, in: Proceedings of ACM MobiCom'03, San Diego, CA, USA, 2003, pp. 161–175.
[19] D.-M. Chiu, R. Jain, Analysis of the increase and decrease algorithms for congestion avoidance in computer networks, Journal of Computer Networks and ISDN Systems 17 (1989).
[20] V. Gambiroza, B. Sadeghi, E.W. Knightly, end-to-end performance and fairness in multihop wireless backhaul networks, in: Proceedings of ACM MobiCom'04, Philadelphia, Pennsylvania, USA, 2004, pp. 287–301.
[21] L. Sang, A. Arora, H. Zhang, On Exploiting asymmetric wireless links via one-way estimation, in: Proceedings of ACM MobiHoc'07, Montréal, Quebéc, Canada, 2007, pp. 11–21.
[22] K. Ramachandran, M. Buddhikot, G. Chandranmenon, S. Miller, E. Belding-Royer, K. Almeroth, On the design and implementation of infrastructure mesh networks, in: Proceedings of IEEE WiMesh'05, Santa Clara, CA, USA, 2005.
[23] S. Biswas, R. Morris, ExOR: opportunistic multi-hop routing for wireless networks, in: Proceedings of ACM SIGCOMM'05, Philadelphia, PA, USA, 2005, pp. 133–144.
[24] S. Chachulski, M. Jennings, S. Katti, D. Katabi, Trading structure for randomness in wireless opportunistic routing, in: Proceedings of ACM SIGCOMM'07, Kyoto, Japan, 2007, pp. 169–180.
[25] S. Miskovic, E.W. Knightly, Routing primitives for wireless mesh networks: design, analysis and experiments, in: Proceedings of IEEE INFOCOM'10, San Diego, CA, USA, 2010.

Seongkwan Kim is a Senior Engineer at Samsung Electronics Co., Ltd., where he is currently working on the design of 4G telecommunications system such as IEEE 802.16e/m Mobile WiMAX. He received his Ph.D. degree in electrical engineering and computer science from Seoul National University in 2009, and received his B.S. and M.S. degrees in electronics engineering from Korea University in 2002 and 2004, respectively. He was with Hewlett-Packard Laboratories, Palo Alto, CA, USA as a visiting scholar in 2006. His research interests include algorithmic design and protocol development for various practical communication systems such as IEEE 802.11/15/16, cognitive radio, sensor/ad hoc network, wireless mesh network, etc. He is a winner of the Best Paper Award in the 28th Korean Institute of Information Scientists and Engineers Student Paper Contest, and the Grand Prize in the 3rd IEEE Student Paper Contest awarded by IEEE Seoul Section. He was a recipient of IEEE Technical Committee on Computer Communications (TCCC) Student Travel Grant Award. He also received a Bronze Prize in the 12th Samsung Humantech Thesis Prize. He is a member of the IEEE.

Okhwan Lee received the B.S. in School of Electronics Engineering from Seoul National University in 2006. He is currently pursuing the Ph.D. degree at the School of Electrical Engineering and Computer Science, Seoul National University, Seoul, Korea. His current research interests in the area of wireless/mobile networks with emphasis on IEEE 802.11-based WLAN wireless mesh networking, MU-MIMO in WLAN, transmission rate control algorithm, user scheduling, design of enhanced MAC protocol, design of wireless mesh routing metric/protocol. He is a student member of the IEEE since 2008.

Sunghyun Choi is an associate professor at the School of Electrical Engineering, Seoul National University (SNU), Seoul, Korea. Before joining SNU in September 2002, he was with Philips Research USA, Briarcliff Manor, New York, USA as a Senior Member Research Staff and a project leader for three years. He was also a visiting associate professor at the Electrical Engineering department, Stanford University, USA from June 2009 to June 2010. He received his B.S. (summa cum laude) and M.S. degrees in electrical engineering from Korea Advanced Institute of Science and Technology (KAIST) in 1992 and 1994, respectively, and received Ph.D. at the Department of Electrical Engineering and Computer Science, The University of Michigan, Ann Arbor in September, 1999.

His current research interests are in the area of wireless/mobile networks with emphasis on wireless LAN/MAN/PAN, next-generation mobile networks, mesh networks, cognitive radios, resource management, data link layer protocols, and cross-layer approaches. He authored/coauthored over 150 technical papers and book chapters in the areas of wireless/mobile networks and communications. He has co-authored (with B. G. Lee) a book "Broadband Wireless Access and Local Networks: Mobile WiMAX and WiFi," Artech House, 2008. He holds 27 US patents, 15 European patents, and 23 Korea patents, and has tens of patents pending. He has served as a General Co-Chair of COMSWARE 2008, and a Technical Program Committee Co-Chair of ACM Multimedia 2007, IEEE WoWMoM 2007 and IEEE/Create-Net COMSWARE 2007. He is currently serving as a Co-Chair of IEEE GLOBECOM 2011 Wireless Networking Symposium, and was a Co-Chair of Cross-Layer Designs and Protocols Symposium in IWCMC 2006, 2007, and 2008, the workshop co-chair of WILLOPAN 2006, the General Chair of ACM WMASH 2005, and a Technical Program Co-Chair for ACM WMASH 2004. He has also served on program and organization committees of numerous leading wireless and networking conferences including ACMMobiCom, IEEE INFOCOM, IEEE SECON, IEEE MASS, and IEEE WoWMoM. He is also currently serving on the editorial boards of IEEE Transactions on Mobile Computing and IEEE Wireless Communications, and has served as an editor of ACM SIGMOBILE Mobile Computing and Communications Review (MC2R), Journal of Communications and Networks (JCN), Computer Networks, and Computer Communications. He has served as a guest editor for IEEE Journal on Selected Areas in Communications (JSAC), IEEE Wireless Communications, Pervasive and Mobile Computing (PMC), ACM Wireless Networks (WINET), Wireless Personal Communications (WPC), and Wireless Communications and Mobile Computing (WCMC). He gave a tutorial on IEEE 802.11 in ACM MobiCom 2004 and IEEE ICC 2005. From 2000 to 2007, he was an active voting

member of IEEE 802.11 WLAN Working Group.

He has received a number of awards including the Young Scientist Award awarded by the President of Korea (2008); IEEK/IEEE Joint Award for Young IT Engineer (2007); the Outstanding Research Award (2008) and the Best Teaching Award (2006) both from the College of Engineering, Seoul National University; the Best Paper Award from IEEE WoWMoM 2008; and Recognition of Service Award (2005, 2007) from ACM. Dr. Choi was a recipient of the Korea Foundation for Advanced Studies (KFAS) Scholarship and the Korean Government Overseas Scholarship during1997–1999 and 1994–1997, respectively. He is a senior member of IEEE, and a member of ACM, KICS, IEEK, KIISE.

Sung-Ju Lee is a senior research scientist at the Networking & Communications Lab of Hewlett-Packard Laboratories in Palo Alto, CA, USA. He received his Ph.D. in Computer Science from the University of California, Los Angeles (UCLA). He has published more than 80 papers and has 11 granted patents in the area of computer networks and distributed systems. His recent research interests include WLANs, large scale wireless sensor networks, network management, and cross layer algorithm design. He is a senior member of IEEE and ACM.